

Broadband return-to-zero wavelength conversion and signal regeneration using a monolithically integrated, photocurrent-driven wavelength converter

M.N. Sysak, L.A. Johansson, J.W. Raring, H.N. Poulsen, D.J. Blumenthal and L.A. Coldren

Broadband wavelength switching and signal regeneration experiments with 10 Gbit/s return-to-zero signals using a photocurrent-driven wavelength converter (PD-WC) are presented. For wavelength switching using an ideal input signal to the PD-WC, the device generates up to +3.7 dB facet to facet gain and shows <1 dB power penalty in bit error rate measurements. For wavelength switching with a degraded input signal, the PD-WC shows extinction ratio regeneration from 5 to >11 dB, jitter reduction from 35 to 17 ps, significant eyeshape regeneration, and a -2.8 dB power penalty.

Introduction: Dynamic wavelength switching and signal regeneration are critical functions to enhance the performance of next generation networks. Of particular importance is a monolithically integrated device that can perform these functions, including signal reamplification, reshaping, retiming (3R) and wavelength conversion with a small form factor. Such a device has the potential for low packaging costs and low coupling losses between discrete components.

Several approaches have been explored for simultaneous wavelength switching and signal regeneration. These include interferometric optical amplifiers, nonlinear fibres, and a variety of electroabsorption modulator (EAM) approaches [1-3]. However, these approaches generally have high loss between components, high power dissipation, or need optical filtering to separate input and regenerated signals. Recently we have demonstrated a small form factor monolithically integrated PD-WC [4]. The high degree of integration allows for low coupling losses, and the separation of input and output signals enables full wavelength transparency without output signal filtering. In this Letter we present optical wavelength switching and 3R regeneration using the PD-WC. The device employs a tandem modulator clock recovery technique [5] to regenerate the degraded optical signals.

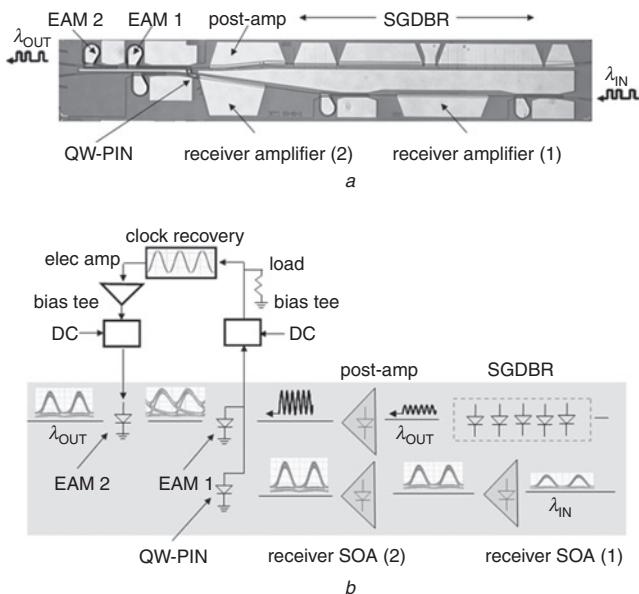


Fig. 1 SEM image of monolithically integrated (3.0 × 0.5 mm) PD-WC, and functional schematic, eye diagrams at various locations in wavelength converter, and clock recovery apparatus used for signal regeneration

a SEM image
b Functional schematic, eye diagrams, clock recovery apparatus

The PD-WC consists of an optically preamplified receiver and a widely tunable transmitter fabricated in a parallel waveguide arrangement as shown in Fig. 1a. The receiver contains two SOAs followed by a quantum well (QW)-PIN photodetector and provides 20 dB gain for transverse electric (TE) polarised input signals. The compressively strained quantum wells used for gain throughout the device make it

polarisation sensitive, with preference for TE polarised signals. The transmitter consists of a sampled grating DBR (SGDBR) laser, an SOA post-amplifier, a 400 μm-long EAM (EAM-1), and an additional 200 μm-long EAM (EAM-2). EAM-1 and the QW-PIN share a common reverse bias applied through a bias tee and a ground-signal probe. An external 50 Ω load resistor is used on the RF side of the bias tee for bandwidth. A 35 μm-long Ti/Pt/Au metal trace connects the QW-PIN photodetector and EAM-1.

For wavelength switching, photocurrent from the receiver is routed over the metal interconnect and used to change the voltage across EAM-1 via the load resistor. The voltage change modulates the transmission characteristics of this EAM which inscribes the input signal onto the output wavelength of the SGDBR. The DC bias applied to EAM-1 and the RF swing from the QW-PIN set the zero level and the gate opening (EAM-1) at the output from the tunable transmitter. For signal reshaping and retiming, the device uses a second EAM (EAM-2) that spatially follows EAM-1 on the transmitter waveguide. The generated photocurrent used to drive EAM-1 is used to trigger an external clock recovery circuit. The clock source is then electrically amplified and fed back to EAM-2 which acts as a pulse carver, gating the shape of the optical signal from EAM-1. Variable delay elements are used to phase match the recovered clock to the data. A functional schematic of the wavelength conversion and clock recovery along with eye diagrams at various points in the device are shown in Fig. 1b.

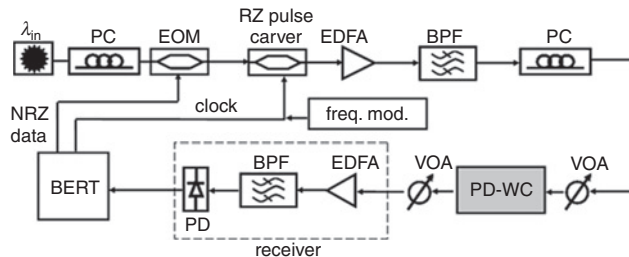


Fig. 2 Experimental setup for regeneration and wavelength switching experiments using PD-WC

NRZ data converted to RZ data using carving Mach-Zehnder modulator over-driven by clock source from BERT. Frequency modulation introduced onto carving modulator using swept frequency source

Experiment: Wavelength switching and signal regeneration were performed using the experimental setup shown in Fig. 2. A non-return-to-zero (NRZ) $2^{31} - 1$ word length pseudorandom bit stream (PRBS) at 10 Gbit/s was generated from a bit error rate tester (BERT) at 1548 nm. To form the RZ data, the NRZ signal is gated using an external carving Mach-Zehnder modulator that is over-driven by the NRZ clock source from the BERT such that it switches from off-to on-state in a single bit period. The RZ optical data signal is then amplified with an EDFA and filtered with a 0.35 nm filter before being coupled to the device using a lensed fibre. After regeneration and wavelength conversion, the output from the device is coupled to another lensed fibre and routed to an optical receiver before either being fed back to the BERT, or to a digital component analyser (DCA). Measurements of the wavelength converted eye diagrams and the converted optical power, ER, and jitter were performed using the DCA. Jitter was added to the input optical signal fed to the PD-WC by introducing a 10 MHz sinusoidal frequency modulation onto the electrical signal driving the carving modulator.

Results: Measurements of the frequency response of the wavelength converting portion of the regenerator (QW-PIN and EAM-1) with a 50 Ω termination showed an optical to optical 3 dB bandwidth of between 6 to 7 GHz. The slightly band-limited characteristics are attractive since the converted pulse becomes spread out in time before entering the carver. This allows more margin for the gating function of EAM-2 to carve out the inside of the converted signal.

For wavelength switching, a 15 dB ER input signal at 1548 nm with -7 dBm fibre coupled on-chip power was fed to the PD-WC. The receiver amplifiers were biased to 6 kA/cm², the transmitter SGDBR gain was biased to 130 mA and the transmitter post-amplifier was biased to 100 mA. The applied bias on EAM-1 and the QW-PIN photodetector was -2.0, -2.6 and -3.0 V for output wavelengths of 1541, 1553 and 1563 nm, respectively. The bias on the carving EAM

was -1.5 V. The amplified clock signal fed back to the carving EAM was $3 V_{pp}$, and was measured after the bias tee before entering the device. For switching from 1548 to 1541, 1553 and 1563 nm, BER measurements are shown in Fig. 3 and show a 1 dB power penalty for converted signals. The converted extinction ratios were 11.3, 11.2 and 11.4 dB, and output power levels were -8.2 , -8 and -7.5 dBm for each of the indicated output wavelengths. After measuring and accounting for the 4.2 dB fibre coupling loss, the facet to facet gain of the device at each of these wavelengths is $+3$, $+3.2$ and $+3.7$ dB.

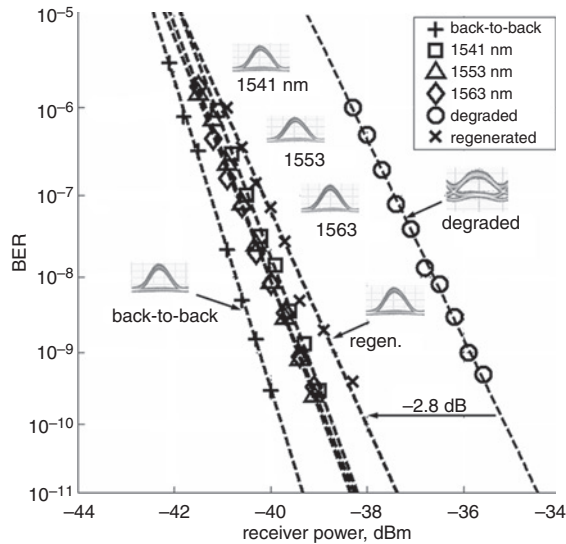


Fig. 3 BER measurements at 10 Gbit/s for wavelength switching using ideal input signal and signal regeneration with degraded input. Receiver amplifier biased to 6 kA/cm^2 ; transmitter laser gain and post-amp SOA biased to 130 and 100 mA, respectively, in all experiments

To demonstrate ER regeneration and eye diagram reshaping, the input to the PD-WC was degraded by rotating the polariser before the carving Mach-Zehnder modulator in Fig. 2. An eye diagram of the degraded input signal at 1548 nm is shown in Fig. 3. The degraded input signal ER was 5 dB, the optical signal-to-noise ratio was 25 dB, and the on-chip input power to the receiver was -7 dBm. Bias conditions in the PD-WC were identical to that used for wavelength switching experiments with an output of 1541 nm. After wavelength conversion to 1545 nm and signal regeneration, the output signal extinction was improved to 11 dB, the fibre coupled output power was -9 dBm, and the output OSNR was 45 dB. BER measurements were performed and we observe a -2.8 dB power penalty between the BER curves for the degraded and regenerated signals.

Jitter reduction experiments were performed by examining input and converted waveforms after adding various amounts of 10 MHz sinusoidal frequency modulation onto the MZ-pulse carving modulator in Fig. 2. Input and output wavelengths were 1548 and 1541 nm, respectively. Converted eye diagrams and measurements of the peak-to-peak jitter are summarised in Fig. 4. Bias conditions on the PD-WC are identical to that used for conversion to 1541 nm, except that the

wavelength converter (EAM-1 and QW-PIN) bias is set to -2.3 V. For input peak-to-peak jitter of 35, 25 and 15 ps, conversion through the device reduced the jitter to 17, 13 and 8 ps, respectively.

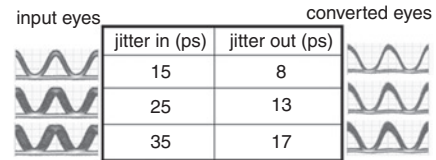


Fig. 4 Wavelength switched input and output eye diagrams with added jitter at input of device

Jitter added as a 10 MHz frequency modulation onto Mach-Zehnder pulse carving modulator outlined in Fig. 2

Conclusion: We have demonstrated a monolithically integrated wavelength converter capable of broadband wavelength switching, facet to facet reamplification, signal reshaping, and signal retiming. For wavelength switching using ideal input signals, the PD-WC provides signal reamplification up to $+3.7$ dB. For degraded input signals, the PD-WC shows reshaping of the converted signal eye diagrams and extinction ratio improvements from 5 to >11 dB. Jitter measurements show jitter reduction from 35 to 18, 25 to 13 and 15 to 8 ps for wavelength switching through the device with added 10 MHz frequency modulation onto the input. BER measurements show -2.8 dB power penalty for degraded waveform signals after regeneration through the PD-WC.

© The Institution of Engineering and Technology 2006
17 August 2006

Electronics Letters online no: 20062415
doi: 10.1049/el:20062415

M.N. Sysak, L.A. Johansson, H.N. Poulsen, D.J. Blumenthal and L.A. Coldren (Electrical and Computer Engineering Department, University of California, Santa Barbara, CA 93106, USA)

E-mail: mnsysak@engineering.ucsb.edu

J.W. Raring (Materials Department, University of California, Santa Barbara, CA 93106, USA)

References

- Schubert, C., *et al.*: '160 Gbit/s wavelength converter with 3R regenerating capability', *Electron. Lett.*, 2002, **38**, (16), pp. 903–904
- Leuthold, J., *et al.*: 'Novel 3R regenerator based on semiconductor optical amplifier delayed-interference configuration', *IEEE Photonics Technol. Lett.*, 2001, **13**, (8), pp. 860–862
- Hu, Z., *et al.*: 'Optical clock recovery circuits using travelling-wave electroabsorption modulator based ring oscillators for 3R regeneration', *IEEE J. Sel. Top. Quantum Electron.*, 2005, **11**, (2), pp. 329–337
- Sysak, M.N., *et al.*: 'Single-chip, widely-tunable 10 Gbit/s photocurrent-driven wavelength converter incorporating a monolithically integrated laser transmitter and optical receiver', *Electron. Lett.*, 2006, **42**, (11), pp. 657–658
- Chou, H.F., and Bowers, J.E.: 'Simplified optoelectronic 3R regenerator using nonlinear electro-optical transformation in an electroabsorption modulator', *Opt. Express*, 2005, **13**, (7), pp. 2742–2746